

KALEIDO: OPEN-SOURCED MULTI-SUBJECT REFER- ENCE VIDEO GENERATION MODEL

000
001
002
003
004
005 **Anonymous authors**
006 Paper under double-blind review
007
008
009
010
011
012
013
014
015
016
017
018
019
020
021
022
023
024
025
026
027
028
029
030
031
032
033
034
035
036
037
038
039
040
041
042
043
044
045
046
047
048
049
050
051
052
053

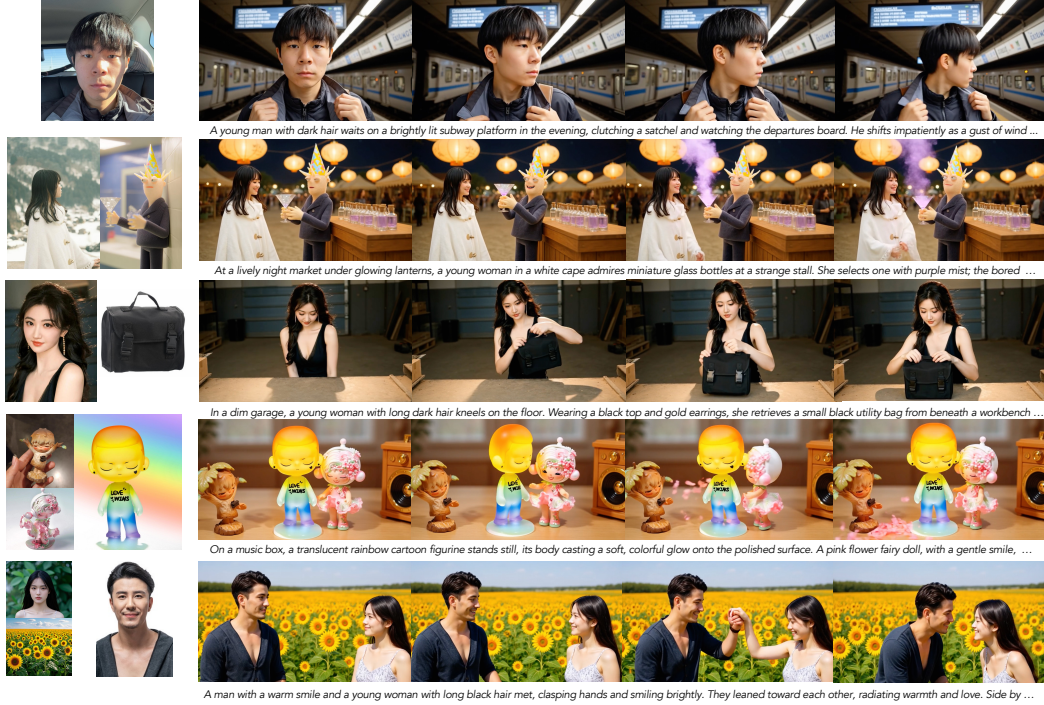


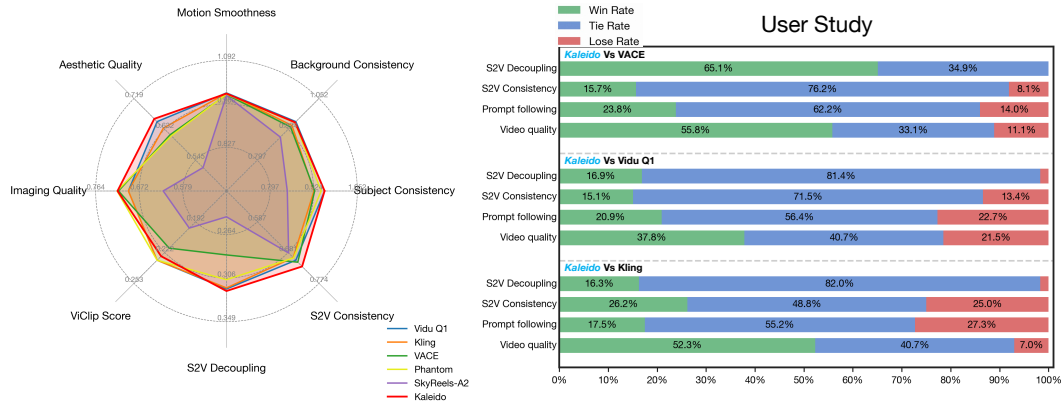
Figure 1: Subject-to-video generation by *Kaleido* covering humans, objects, and controlled backgrounds in both single and multi-subject cases.

ABSTRACT

We present *Kaleido*, a subject-to-video (S2V) generation framework, which aims to synthesize subject-consistent videos conditioned on multiple reference images of target subjects. Despite recent progress in S2V generation models, existing approaches remain inadequate at maintaining multi-subject consistency and at handling background disentanglement, often resulting in lower reference fidelity and semantic drift under multi-image conditioning. These shortcomings can be attributed to several factors. Primarily, the training dataset suffers from a lack of diversity and high-quality samples, as well as cross-paired data, i.e., paired samples whose components originate from different instances. In addition, the current mechanism for integrating multiple reference images is suboptimal, potentially resulting in the confusion of multiple subjects. To overcome these limitations, we propose a dedicated data construction pipeline, incorporating low-quality sample filtering and diverse data synthesis, to produce consistency-preserving training data. Moreover, we introduce Reference Rotary Positional Encoding (R-RoPE) to process reference images, enabling stable and precise multi-image integration. Extensive experiments across numerous benchmarks demonstrate that *Kaleido* significantly outperforms previous methods in consistency, fidelity, and generalization, marking an advance in S2V generation. The source code and trained model checkpoints for this study are available at [here](#).

054 1 INTRODUCTION

056 Recent years have witnessed rapid and highly promising advances in video generation. Inspired in
 057 part by the success of Sora, diffusion models integrated with Diffusion Transformers (DiT) (Peebles
 058 & Xie, 2023; Esser et al., 2024) have emerged as a prevailing paradigm and get further developed.
 059 Commercial models like Veo3 (DeepMind) and Kling (Kuaishou) have already achieved video qual-
 060 ity on par with professional production standards, introducing a new workflow paradigm for video
 061 content creation that greatly improves efficiency while reducing production costs. In the open-source
 062 domain, models such as Wan (Wang et al., 2025) and CogVideoX (Yang et al., 2025) not only share
 063 these advantages, but also facilitate customized fine-tuning for specific applications.



078 Figure 2: Subject-to-video evaluation (left) and user study results comparing *Kaleido* with VACE,
 079 Kling, and Vidu-Q1 (right).

082 Current pretraining video generation research primarily focuses on two major tasks: text-to-
 083 video (T2V) and image-to-video (I2V) generation. The former synthesizes videos directly from
 084 textual descriptions, often yielding content with high creative diversity but also considerable ran-
 085 domness. The latter transforms a static image into a dynamic video, imposing a strict constraint of
 086 identical first frame, which tends to limit creative flexibility. Consequently, the need for more flex-
 087 ible control over video generation has grown increasingly strong. **Subject-to-video (S2V) genera-
 088 tion**, which aims to synthesize subject-consistent videos conditioned on multiple reference images
 089 of target subjects, has attracted rising attention. Commercial systems such as Vido (Bao et al., 2024)
 090 and Kling (Kuaishou) exemplify this trend, demonstrating substantial potential in industries such as
 091 e-commerce and advertising.

092 The S2V task requires decoupling target subjects from given reference images and generating videos
 093 according to textual prompts, while maintaining the appearance of the subjects consistently. The
 094 subjects encompass a wide range of visual entities, including humans, objects, and backgrounds.
 095 It unifies the creativity of T2V generation and the controllability of I2V generation, enabling more
 096 flexible control in video generation.

097 However, existing open-source S2V models remain inferior to their closed-source counterparts. This
 098 gap is primarily reflected in the difficulty of maintaining consistent visual appearances across diverse
 099 subject compositions, as well as in producing high-quality videos. This performance gap can be
 100 primarily attributed to two fundamental challenges:

- 101 • **Lack of effective training data.** In most recent data construction pipelines, reference im-
 102 ages are naively selected from video frames. Models trained on such data often tend to
 103 completely replicate the subjects in reference images (without altering their viewpoints,
 104 poses, or other dynamic attributes), rather than decoupling the subjects and focusing on
 105 their intrinsic characteristics. Consequently, generated videos may inherit extraneous el-
 106 ements, such as superfluous background details or irrelevant objects present in the refer-
 107 ence images, which are usually undesirable in videos. Furthermore, existing models often
 108 struggle to preserve satisfactory consistency in various scenarios, including multi-subject

108 compositions or scenes involving animated characters. This limitation is largely due to the
 109 insufficient coverage and quality of training data.
 110

- 111 • **Inadequate conditioning strategies.** Current strategies for incorporating reference image
 112 information into the generation pipeline are generally suboptimal, hindering the model’s
 113 ability to efficiently capture and represent the subject’s characteristics. For example, Phan-
 114 tom (Liu et al., 2025) adopts latent feature concatenation along the sequence dimension,
 115 while this method may cause different reference objects to overlap spatially, leading to
 116 undesirable compositional artifacts. VACE (Jiang et al., 2025) employs an adapter-based
 117 architecture, but it needs a non-negligibly additional inference cost.

118 We introduce a set of methods that allow open-source models to attain performance on par with
 119 closed-source counterparts. Our contributions can be summarized as follows:
 120

- 121 • **A comprehensive data construction pipeline.** Our data pipeline employs multi-class sam-
 122 pling, stringent filters, and cross-paired data construction to enrich subject and scene di-
 123 versity, elevate overall data fidelity, and ensure subjects are disentangled from extraneous
 124 elements.
- 125 • **An effective image condition injection method**, dubbed R-Rope, which introduces rotary
 126 position encoding for subject tokens to maximize the model’s ability to integrate informa-
 127 tion from multiple reference images. This mechanism improves multi-image and multi-
 128 subject S2V consistency, while maintaining computational efficiency.
- 129 • **A state-of-the-art (SOTA) open-source S2V model.** Extensive experiments show that our
 130 approach achieves excellent S2V performance in terms of subject fidelity, background dis-
 131 entanglement, and general generation quality, substantiating its effectiveness for building
 132 general-purpose, subject-consistent video generation models.

133 Furthermore, we will **open-source** both our **data pipeline** and **pretrained S2V model** to support
 134 the community and provide a strong foundation for future research on subject-to-video generation.
 135

137 2 RELATED WORK

139 Reference-guided generation has been widely studied in both image and video domains. In the
 140 image domain, methods such as DreamBooth (Ruiz et al., 2023) explored personalized generation
 141 by fine-tuning diffusion models on a small set of reference images, enabling the preservation of
 142 subject-specific characteristics. Extensions such as IP-Adapter (Ye et al., 2023) further enhanced
 143 reference conditioning by leveraging multiple input images and contextual information, although
 144 these works remain limited to static image synthesis. In parallel, video generation has undergone a
 145 rapid evolution: GAN-based approaches (Goodfellow et al., 2014) initially struggled with stability
 146 and temporal coherence, while diffusion models based on U-Net architectures introduced notable
 147 improvements in quality. More recently, Diffusion Transformers have brought substantial progress
 148 in controllability, text alignment, and long-range temporal consistency, giving rise to a variety of
 149 downstream tasks including video editing, video inpainting, and text-to-video generation.

150 Building upon these advances, the subject-to-video (S2V) task has emerged as a natural exten-
 151 sion of reference-guided generation. Proprietary systems such as Vido (Bao et al., 2024) and
 152 Kling (Kuaishou) demonstrated the feasibility of generating videos from reference images, attract-
 153 ing significant attention but limiting community access due to their closed-source nature. The sub-
 154 sequent release of open-source frameworks such as VACE (Jiang et al., 2025), Phantom (Liu et al.,
 155 2025) and SkyReels-A2 (Fei et al., 2025) accelerated research in this field, enabling applications
 156 ranging from digital human generation to virtual try-on and face-swapping. Despite these develop-
 157 ments, existing S2V models (Jiang et al., 2024; Zhou et al., 2024; Wang et al., 2024) still face per-
 158 sistent challenges. In particular, many approaches rely on directly concatenating reference embeddings
 159 with video latents, which often leads to insufficient background disentanglement and degraded sub-
 160 ject fidelity. When the reference subject appears in complex backgrounds, models frequently carry
 161 over background artifacts into the generated video. Moreover, in multi-subject or multi-image set-
 162 tings, the lack of dedicated mechanisms for reference alignment commonly results in token disorder
 163 and weakened temporal consistency.

162 Our work builds on these foundations while addressing the limitations of prior S2V approaches.
 163 By introducing a more comprehensive data pipeline and improved training strategies, we aim to
 164 enhance both background disentanglement and subject fidelity, moving toward a more general and
 165 robust framework for subject-aware video generation.
 166

167 3 DATASET CONSTRUCTION PIPELINE

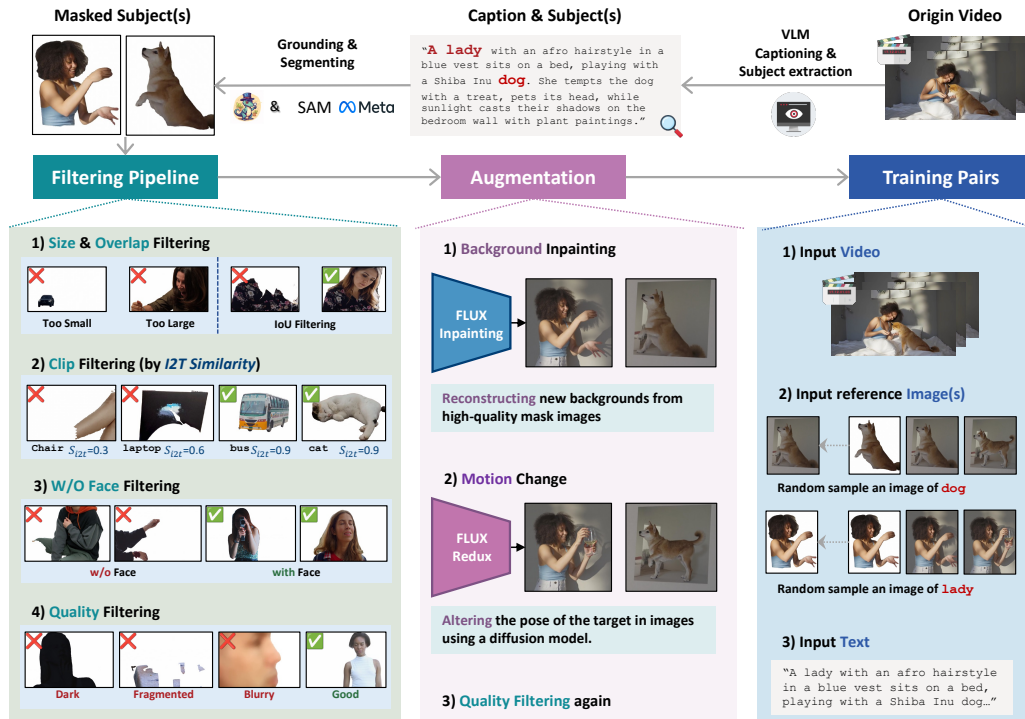
168 3.1 MOTIVATION

169 Subject-to-Video (S2V) generation addresses the challenge of synthesizing videos of a specific sub-
 170 ject, conditioned on reference images and textual prompts. Achieving high-quality S2V in broad
 171 open-world scenarios relies on the availability of training data that is diverse in content and consists
 172 strictly of decoupled image-video pairs. In such pairs, the visual attributes of the subject must be
 173 independent of the surrounding context.
 174

175 Previous work primarily utilizes datasets designed for subject-driven image generation or limited
 176 video tasks, which do not adequately meet these requirements. This leads to three significant limitations:
 177 a lack of subject and scene diversity hinders generalizability; inconsistent annotation quality
 178 decreases controllability; and image-video pairs are entangled with background information. Con-
 179 sequently, current S2V models often rely on separate segmentation or subject extraction steps during
 180 inference, preventing true end-to-end subject conditioning and restricting compositional flexibility.
 181

182 To address these constraints and facilitate the development of genuinely end-to-end S2V models ap-
 183 plicable in unconstrained scenarios, we propose a new dataset construction pipeline. Our approach
 184 incorporates robust grounding and segmentation, along with advanced filtering techniques and a
 185 cross-paired composition strategy designed to enforce subject-background disentanglement at scale.
 186 This process produces diverse, high-quality data pairs essential for training models capable of di-
 187 rectly synthesizing videos from unsegmented reference images and flexible prompts, thus advancing
 188 S2V research towards practical deployment in open-domain applications.
 189

190 3.2 PIPELINE DESIGN



215 Figure 3: Scalable multi-stage data pipeline for subject-to-video (S2V) generation, where data aug-
 216 mentation enables the creation of cross-paired samples for robust training.

216 To achieve these objectives, we propose a scalable, multi-stage dataset construction pipeline 3 tailored to the needs of S2V. The process is summarized as follows:
 217
 218

219 **(1) Video Preprocessing and Captioning.** We start by slicing large-scale raw video collections
 220 into shorter clips, each containing coherent actions or events. An automatic captioning model generates
 221 textual descriptions for each clip, ensuring alignment between the visual and textual modalities.
 222

223 **(2) Subject Category Definition and Candidate Identification.** To further enhance diversity, we
 224 construct a broad taxonomy of subject categories covering various domains (e.g., humans, objects,
 225 backgrounds). This taxonomy comprises over 100 distinct subject categories and includes over 800
 226 candidate synonyms and instances, enabling captions to be matched against a rich vocabulary to
 227 identify candidate subjects ($class_v$) for further processing. This method enables scalable subject
 228 discovery without manual annotation, thus enriching the dataset with diverse subjects.
 229

230 **(3) Grounding and Segmentation.** For accurate localization of subject regions, we employ
 231 Grounding DINO (Liu et al., 2024) for robust localization and SAM (Kirillov et al., 2023) for fine-
 232 grained segmentation. This combination ensures both semantic correctness and boundary precision,
 233 which are essential for effective subject-centric video generation.
 234

235 **(4) Filtering and Validation.** To guarantee data quality, we implement several filtering strategies:
 236 (i) **Size Filtering:** Removes excessively small or large instances; (ii) **CLIP-Based Classification:**
 237 Verifies category alignment against textual descriptions; (iii) **IoU-Based Filtering:** Excludes instances
 238 with significant overlapping regions, ensuring distinct subject representation; and (iv) **Quality Checks:**
 239 Brightness and blur assessments filter out low-quality samples. For human categories, we use InsightFace
 240 to retain only instances with valid frontal faces, enhancing identity preservation.
 241

242 **(5) Augmentation via Background Disentanglement.** One of the key challenges in S2V is the en-
 243 tanglement of subject and background. To mitigate this issue, we apply inpainting techniques (Labs
 244 et al., 2025) to segmented regions in the reference images, effectively erasing background information.
 245 During training, the model is encouraged to reconstruct subject appearances from the reference
 246 images while relying on textual prompts for background synthesis. This strategy prevents overfitting
 247 to incidental background cues and enhances subject transferability across various scenes.
 248

249 **(6) Augmentation via Pose and Motion Enrichment.** Finally, to improve diversity and avoid
 250 overfitting to frame-level similarity, we utilize Flux Redux (Labs et al., 2025) to enrich reference
 251 images with novel poses and motions not present in the original video frames. This enhancement
 252 encourages the model to learn a more generalizable representation of subject identity that is robust
 253 to motion variations.
 254

255 The resulting pipeline not only yields high-quality, background-independent subject annotations, but
 256 also provides a versatile framework applicable to a wide range of downstream applications. More
 257 importantly, it establishes a unified perspective on S2V, laying the groundwork for future research
 258 focused on subject-specific personalization and multi-task unification.
 259

260 4 FRAMEWORK

261 We explore an innovative framework for video generation based on diffusion models. Our primary
 262 focus is on integrating multiple reference images to improve the video generation process. Given a
 263 set of reference images I_1, I_2, \dots, I_n , a textual input T , and the target video V , our objective can be
 264 formulated as follows.
 265

$$V = \mathcal{G}(I_1, I_2, \dots, I_n, T; z) \quad (1)$$

266 where z represents the stochastic noise variable intrinsic to the video generation process. The goal is
 267 for V to be visually coherent, effectively encapsulating information from the reference images and
 268 adhering to textual guidance.
 269

270 4.1 PRELIMINARIES

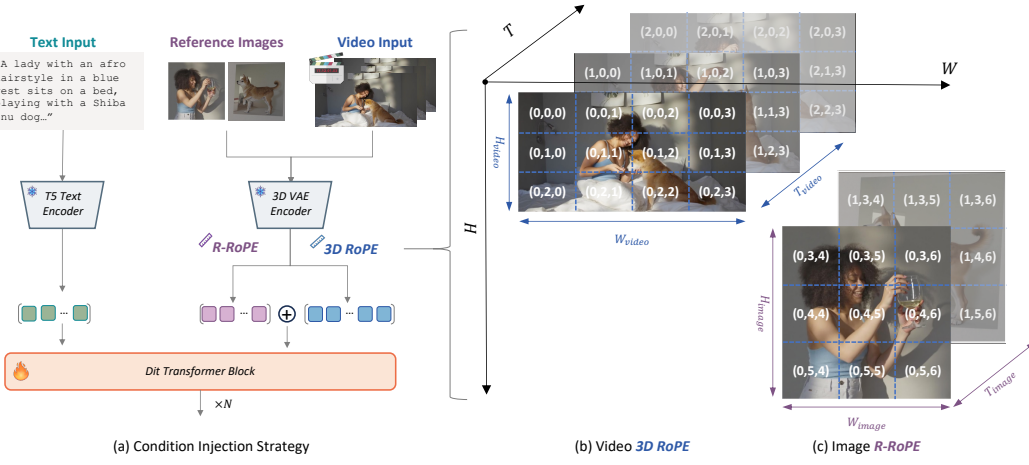
271 Text-to-video (T2V) synthesis extends diffusion-based modeling into the spatio-temporal domain,
 272 aiming to transform Gaussian noise variables $\epsilon \sim \mathcal{N}(0, I)$ into coherent videos \mathbf{x}_0 that correspond
 273 to a target sequence of frames $\mathbf{x}_1, \mathbf{x}_2, \dots, \mathbf{x}_T$.
 274

270 to a textual description. Modern approaches employ latent diffusion schemes, where a spatio-
 271 temporal autoencoder $E(\cdot)$ compresses videos into a compact latent tensor $Z \in \mathbb{R}^{T \times C \times H \times W}$, with
 272 T denoting the temporal dimension, $H \times W$ the spatial resolution, and C the channel dimension.
 273 Within this latent space, transformer-based denoising networks v_θ iteratively remove noise, lever-
 274 aging spatio-temporal self-attention and relative positional encodings (e.g., 3D Rotary Positional
 275 Embeddings) to capture long-range dependencies. Text conditioning is incorporated by encoding
 276 prompts through a pretrained encoder $\tau_\theta(y)$, with fusion between latent video and text features via
 277 cross-attention layers. For training, we adopt Flow Matching (Esser et al., 2024), where noise is
 278 injected as $x_t = (1 - t)x_0 + t\epsilon$, and the model is optimized with the loss.

$$279 \mathcal{L} = \mathbb{E}_{\mathbf{x}_0, t, y, v} [\|v - v_\theta(E(\mathbf{x}_0), t, \tau_\theta(y))\|_2^2], \quad (2)$$

280 where t is the diffusion timestep, and $v = \frac{dx}{dt} = \epsilon - x_0$.

282 4.2 METHOD



299 Figure 4: Illustration of our subject-to-video framework. (a) Multiple reference images are injected
 300 for guided video generation. (b) Video tokens use 3D RoPE positional encoding, while (c) reference
 301 images utilize **R-RoPE** for distinct spatial-temporal positioning.

303 In this work, we adopt a straightforward condition injection strategy to combine image conditions
 304 with video sequences for S2V tasks. Rather than employing complex adapter-based modules, we
 305 utilize a simple concatenation scheme to merge the encoded image conditions and video noise rep-
 306 resentations along the sequence dimension. Specifically, the input sequence is formulated as:

$$307 X = [I_1, I_2, \dots, I_n, z] \quad (3)$$

309 This approach preserves the inherent structure of the original base model and enables efficient, sta-
 310 ble learning by minimizing architectural modifications. However, direct concatenation with adjacent
 311 position ids introduces a new challenge: the model may misinterpret image conditions as consecu-
 312 tive frames within the video sequence, potentially disrupting temporal continuity and degrading the
 313 quality of the generated video. To address this, **it is essential for the model to differentiate image**
 314 **tokens from video tokens and fully understand their respective roles.**

315 To facilitate this distinction, we introduce the **Reference Rotary Positional Encoding (R-RoPE)**
 316 mechanism. As illustrated in Figure 4, conventional 3D RoPE encodes video tokens using positional
 317 vectors in the form (t, h, w) , where t is the temporal frame index and h, w denote spatial dimensions,
 318 each starting from zero. For image conditions, we modify the positional vectors so that their spa-
 319 tial dimensions are shifted to start from the maximum observed dimensions of the video sequence
 320 (H_{max}, W_{max}), ensuring that image tokens occupy distinct positions and are easily separable from
 321 video tokens within the model’s spatial-temporal embedding space. Furthermore, the temporal posi-
 322 tions of image conditions are individually assigned, beginning from $t = 0$ for each image. Formally,
 323 the positional vectors for each image I_i is defined as:

$$324 \text{Pos}_i = [i - 1, H_{max} : shiftH, W_{max} : shiftW] \quad (4)$$

324	Vidu Q1	Kling	VACE	Phantom	SkyReels	Kaleido
325	<i>Closed-source</i>					
326	<i>Open-source</i>					
<i>General Video Quality Metrics</i>						
327	Subject Consistency	0.956	0.925	0.927	0.946	0.847
328	Background Consistency	0.956	0.940	0.934	0.952	0.892
329	Motion Smoothness	0.993	<u>0.992</u>	0.988	0.989	0.985
330	Aesthetic Quality	0.654	0.636	0.617	0.614	0.524
331	Imaging Quality	0.695	0.695	0.709	0.719	0.621
332	<i>Text-Alignment Metric</i>					
333	ViClip Score	<u>0.230</u>	<u>0.230</u>	0.218	0.231	0.198
334	<i>S2V-Specific Metrics</i>					
335	S2V Decoupling	<u>0.317</u>	0.316	0.284	0.308	0.247
336	S2V Consistency	0.704	0.696	<u>0.710</u>	0.697	0.682
337						

339 Table 1: Quantitative results on S2V generation. Our Kaleido achieves performance across general
 340 metrics. On task-specific metrics, **S2V Consistency** and **S2V Decoupling**, Kaleido attains the best
 341 scores, demonstrating superior subject preservation and irrelevant information disentanglement.

342 where i indexes the image conditions, and shiftH , shiftW indicate the sum of H_{\max} and the height
 343 of the reference image, and the sum of W_{\max} and the width of the reference image, respectively. This
 344 explicit separation in the positional encoding prevents mixing of spatial relationships between the
 345 video sequence and the injected image conditions. By leveraging this concatenation-based condition
 346 injection and positional encoding, our model distinguishes between video and image information
 347 and generates consistent, high-quality video output within the Diffusion Transformer architecture.

349 5 EXPERIMENTS

351 5.1 IMPLEMENTATION DETAILS

352 Our model is fine-tuned from Wan2.1-T2V-14B through a two-stage training paradigm. The pre-
 353 training stage uses **2M** pairs for 10K steps with a learning rate of 1e-5 and batch size of 256, followed
 354 by supervised fine-tuning (SFT) on **0.5M** pairs for 5K steps with the learning rate reduced to 5e-6.
 355 Training is performed with the AdamW optimizer (Kingma & Ba, 2015), leveraging Fully Sharded
 356 Data Parallel (FSDP) and Sequence Parallelism to maximize efficiency.

358 5.2 EVALUATION METRICS

360 To comprehensively evaluate S2V generation, we consider metrics in three aspects. For overall video
 361 quality, we use five standard measures from VBench (Huang et al., 2024): subject consistency, back-
 362 ground consistency, motion smoothness, aesthetic quality, and imaging quality. Semantic alignment
 363 with prompts is assessed using the ViCLIP (Wang et al., 2023) score.

364 We further introduce two dedicated metrics for reference-image correspondence: **S2V Consistency**:
 365 measures how well the subject identity from the reference images is preserved in the generated video.
 366 Subjects are detected and segmented using Grounding Dino and Segment Anything; CLIP features
 367 are extracted, and for each frame the maximum similarity with reference images is computed and
 368 averaged. **S2V Decoupling**: evaluates the model’s ability to disentangle background information.
 369 The subject regions are masked out in both reference images and video frames; CLIP features are
 370 extracted from the backgrounds, and the score is defined as $1 - \text{similarity}$ (higher is better).

371 To ensure robust evaluation, we construct a diverse test set covering humans, animals, cartoons, and
 372 objects, including 400 high-quality reference images and over 170 multisubject cases. These metrics
 373 together provide a comprehensive and balanced assessment of our model’s performance.

375 5.3 MAIN RESULTS

376 **Quantitative Results** Table 1 summarizes the quantitative comparison of our method against both
 377 closed-source and open-source models. Across the five conventional metrics adopted from VBench,

378 our model achieves competitive performance, particularly excelling in *Subject Consistency* and *Aesthetic Quality*. In terms of motion smoothness, background consistency, and imaging quality, our
 379 method closely matching top closed-source models.
 380

381 For task-specific metrics, our method demonstrates clear advantages. We obtain the highest score
 382 on *S2V Consistency* (0.723) and *S2V Decoupling* (0.319), indicating that our model more faithfully
 383 preserves subject identity from reference images while better disentangling background information.
 384 These results highlight the effectiveness of our data construction strategy and architectural design
 385 for handling subject-to-video generation.
 386

387 In addition to automatic metrics, we conduct a user study evaluating four key aspects: Video Quality,
 388 Prompt Alignment, S2V Consistency and S2V decoupling. As illustrated in Figure 2, human raters
 389 consistently prefer our *Kaleido* model over both open-source and closed-source models. Notably,
 390 *Kaleido* achieves the highest ratings in *Video Quality*, *S2V Consistency*, and *S2V Decoupling*, further
 391 confirming the superiority of our approach from a human-centric perspective.
 392

Qualitative Results As shown in Figure 5, we present qualitative comparisons across several repre-
 393

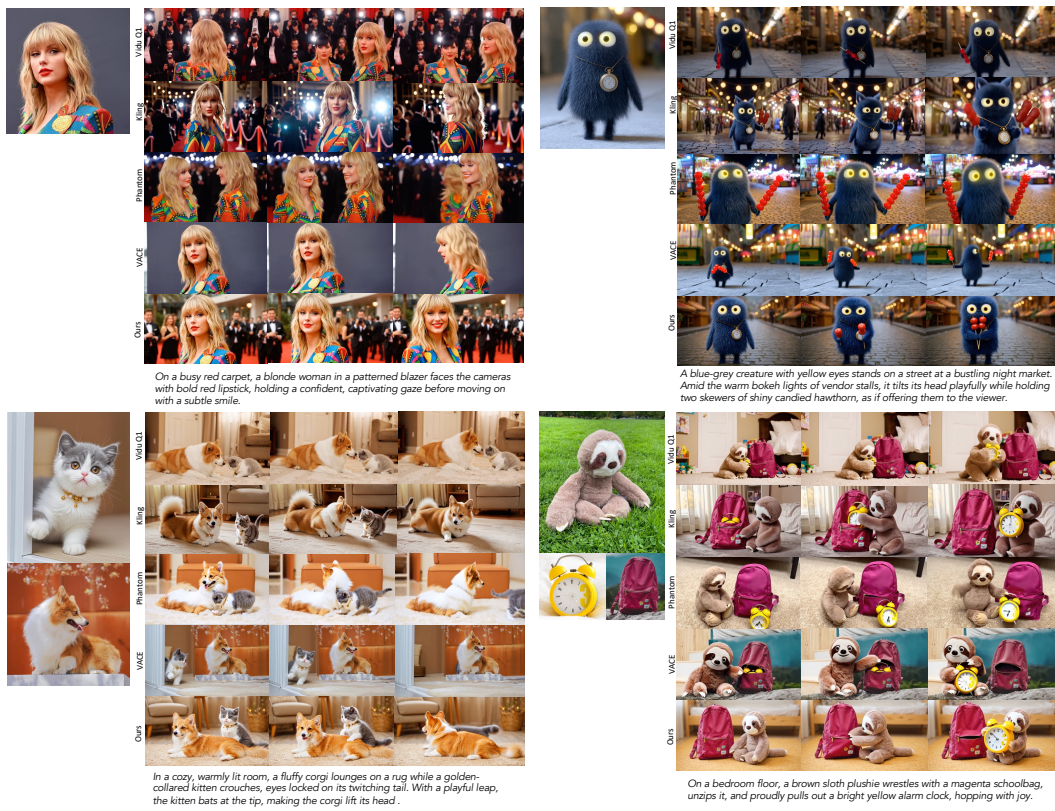


Figure 5: Qualitative comparisons , *Kaleido* clearly demonstrates superior capabilities on **S2V Decoupling**, **S2V Consistency** and **Video Quality**.

sentative scenarios. The results reveal that VACE struggles to disentangle irrelevant information, as background elements from the reference images consistently appear in the generated videos. Vidu, on the other hand, occasionally introduces redundant repetitions of reference images, causing certain subjects to appear multiple times within the generated video. Phantom exhibits similar issues and further suffers from slightly lower overall video quality. In contrast, both Kling and our model outperform other approaches in terms of S2V consistency and disentanglement of irrelevant information. However, Kling occasionally produces errors in reference fidelity—for example, in the animal case, where a small dog is incorrectly rendered with a bell around its neck. Overall, our method achieves a more balanced performance across multiple dimensions, demonstrating substantially stronger disentanglement capability while attaining S2V Consistency comparable to that of closed-source models.

	Concat	ShiftW	ShiftH	ShiftW&H
S2V Consistency	0.661	0.679	0.687	0.708
S2V Decoupling	0.296	0.297	0.304	0.310

Table 2: Ablation: Comparison of R-RoPE Positional Encoding Variants.

5.4 ABLATION STUDY

We conduct comprehensive ablation studies to evaluate the effects of key components in our methodology. Specifically, we analyze the impact of cross-paired data construction on subject-relevant disentanglement and the influence of our proposed R-RoPE positional encoding strategy.

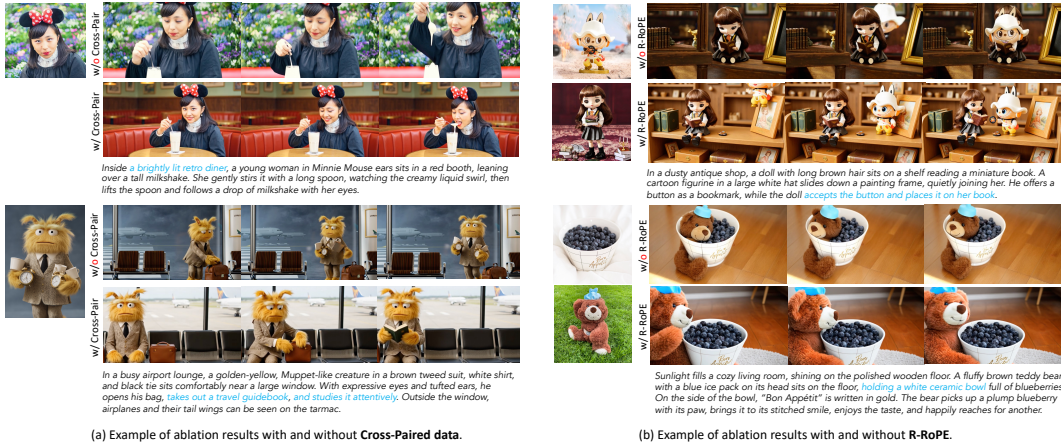


Figure 6: Ablation visualizations. (a) Effect of Cross-Paired data. (b) Effect of R-RoPE.

Effect of Cross-Paired Data Construction. To assess the contribution of Cross-Paired data construction to disentangling subject-specific and irrelevant information, we compare models trained with and without this data. As shown in Table 3, excluding Cross-Paired data leads to a notable decrease in both S2V Consistency and S2V Decoupling metrics, demonstrating its effectiveness. Figure 6a further illustrates that Cross-Paired data training enables the model to better separate the subject from unrelated elements, such as backgrounds and handheld objects. This promotes generation of diverse backgrounds while maintaining focus on the subject, thus facilitating robust decoupling between subject and irrelevant information representations.

Effect of R-RoPE Positional Encoding. We further ablate the proposed R-RoPE positional encoding by considering four settings: (1) baseline (without R-RoPE), (2) shifting only width (ShiftW), (3) shifting only height (ShiftH), and (4) shifting both width and height (ShiftWH). As reported in Table 2, simultaneous spatial shifts result in the highest subject consistency and irrelevant information decoupling. Furthermore, Figure 6 demonstrates that R-RoPE mitigates reference confusion and subject overlap in multi-subject scenarios. These findings confirm that our R-RoPE design is essential for enhancing multi-reference integration and preventing reference-token misalignment during generation.

6 CONCLUSION

In this work, We introduced **Kaleido**, a subject-to-video generation framework to addresses the challenges of multi-subject consistency and background disentanglement under multi-image conditioning. By constructing a diverse and high-quality training dataset with cross-paired samples, and by proposing the R-RoPE positional encoding strategy, Kaleido achieves superior subject preservation and irrelevant information separation, outperforming open-source models and approaching closed-source models.

	w/ Cross-Paired	w/o Cross-Paired
S2V Consistency	0.708	0.670
S2V Decoupling	0.310	0.297

Table 3: Ablation: Impact of Cross-Paired Data Inclusion.

486 REFERENCES
487

488 Fan Bao, Chendong Xiang, Gang Yue, Guande He, Hongzhou Zhu, Kaiwen Zheng, Min Zhao,
489 Shilong Liu, Yaole Wang, and Jun Zhu. Vidu: a highly consistent, dynamic and skilled text-to-
490 video generator with diffusion models. *arXiv preprint arXiv:2405.04233*, 2024.

491 DeepMind. Veo3. <https://deepmind.google/models/veo>.

492

493 Patrick Esser, Sumith Kulal, Andreas Blattmann, Rahim Entezari, Jonas Müller, Harry Saini, Yam
494 Levi, Dominik Lorenz, Axel Sauer, Frederic Boesel, Dustin Podell, Tim Dockhorn, Zion English,
495 and Robin Rombach. Scaling rectified flow transformers for high-resolution image synthesis.
496 In *Forty-first International Conference on Machine Learning, ICML 2024, Vienna, Austria,
July 21-27, 2024*. OpenReview.net, 2024. URL <https://openreview.net/forum?id=FPnUhsQJ5B>.

497

498 Zhengcong Fei, Debang Li, Di Qiu, Jiahua Wang, Yikun Dou, Rui Wang, Jingtao Xu, Mingyuan
499 Fan, Guibin Chen, Yang Li, and Yahui Zhou. Skyreels-a2: Compose anything in video diffusion
500 transformers. *CoRR*, abs/2504.02436, 2025. doi: 10.48550/ARXIV.2504.02436. URL <https://doi.org/10.48550/arXiv.2504.02436>.

501

502

503 Ian J. Goodfellow, Jean Pouget-Abadie, Mehdi Mirza, Bing Xu, David Warde-Farley, Sherjil Ozair,
504 Aaron C. Courville, and Yoshua Bengio. Generative adversarial networks. *CoRR*, abs/1406.2661,
505 2014. URL <http://arxiv.org/abs/1406.2661>.

506

507 Ziqi Huang, Yinan He, Jiashuo Yu, Fan Zhang, Chenyang Si, Yuming Jiang, Yuanhan Zhang, Tianxing
508 Wu, Qingyang Jin, Nattapol Chanpaisit, Yaohui Wang, Xinyuan Chen, Limin Wang, Dahua
509 Lin, Yu Qiao, and Ziwei Liu. Vbench: Comprehensive benchmark suite for video generative
510 models. In *IEEE/CVF Conference on Computer Vision and Pattern Recognition, CVPR 2024,
Seattle, WA, USA, June 16-22, 2024*, pp. 21807–21818. IEEE, 2024. doi: 10.1109/CVPR52733.
511 2024.02060. URL <https://doi.org/10.1109/CVPR52733.2024.02060>.

512

513 Yuming Jiang, Tianxing Wu, Shuai Yang, Chenyang Si, Dahua Lin, Yu Qiao, Chen Change Loy, and
514 Ziwei Liu. Videobooth: Diffusion-based video generation with image prompts. In *IEEE/CVF
515 Conference on Computer Vision and Pattern Recognition, CVPR 2024, Seattle, WA, USA, June
16-22, 2024*, pp. 6689–6700. IEEE, 2024. doi: 10.1109/CVPR52733.2024.00639. URL <https://doi.org/10.1109/CVPR52733.2024.00639>.

516

517 Zeyinzi Jiang, Zhen Han, Chaojie Mao, Jingfeng Zhang, Yulin Pan, and Yu Liu. VACE: all-in-one
518 video creation and editing. *CoRR*, abs/2503.07598, 2025. doi: 10.48550/ARXIV.2503.07598.
519 URL <https://doi.org/10.48550/arXiv.2503.07598>.

520

521 Diederik P. Kingma and Jimmy Ba. Adam: A method for stochastic optimization. In Yoshua
522 Bengio and Yann LeCun (eds.), *3rd International Conference on Learning Representations, ICLR
523 2015, San Diego, CA, USA, May 7-9, 2015, Conference Track Proceedings*, 2015. URL <http://arxiv.org/abs/1412.6980>.

524

525 Alexander Kirillov, Eric Mintun, Nikhila Ravi, Hanzi Mao, Chloe Rolland, Laura Gustafson, Tete
526 Xiao, Spencer Whitehead, Alexander C Berg, Wan-Yen Lo, et al. Segment anything. In *Proceedings
527 of the IEEE/CVF international conference on computer vision*, pp. 4015–4026, 2023.

528

529 Kuaishou. Kling. <https://kling.kuaishou.com/en>.

530

531 Black Forest Labs, Stephen Batifol, Andreas Blattmann, Frederic Boesel, Saksham Consul, Cyril
532 Diagne, Tim Dockhorn, Jack English, Zion English, Patrick Esser, Sumith Kulal, Kyle Lacey,
533 Yam Levi, Cheng Li, Dominik Lorenz, Jonas Müller, Dustin Podell, Robin Rombach, Harry Saini,
534 Axel Sauer, and Luke Smith. FLUX.1 kontext: Flow matching for in-context image generation
535 and editing in latent space. *CoRR*, abs/2506.15742, 2025. doi: 10.48550/ARXIV.2506.15742.
536 URL <https://doi.org/10.48550/arXiv.2506.15742>.

537

538 Lijie Liu, Tianxiang Ma, Bingchuan Li, Zhuowei Chen, Jiawei Liu, Qian He, and Xinglong
539 Wu. Phantom: Subject-consistent video generation via cross-modal alignment. *CoRR*,
abs/2502.11079, 2025. doi: 10.48550/ARXIV.2502.11079. URL <https://doi.org/10.48550/arXiv.2502.11079>.

540 Shilong Liu, Zhaoyang Zeng, Tianhe Ren, Feng Li, Hao Zhang, Jie Yang, Qing Jiang, Chunyuan
 541 Li, Jianwei Yang, Hang Su, et al. Grounding dino: Marrying dino with grounded pre-training
 542 for open-set object detection. In *European conference on computer vision*, pp. 38–55. Springer,
 543 2024.

544 William Peebles and Saining Xie. Scalable diffusion models with transformers. In *IEEE/CVF
 545 International Conference on Computer Vision, ICCV 2023, Paris, France, October 1-6, 2023*, pp.
 546 4172–4182. IEEE, 2023. doi: 10.1109/ICCV51070.2023.00387. URL <https://doi.org/10.1109/ICCV51070.2023.00387>.

547 Nataniel Ruiz, Yuanzhen Li, Varun Jampani, Yael Pritch, Michael Rubinstein, and Kfir Aberman.
 548 Dreambooth: Fine tuning text-to-image diffusion models for subject-driven generation. In *Pro-
 549 ceedings of the IEEE/CVF conference on computer vision and pattern recognition*, pp. 22500–
 550 22510, 2023.

551 Ang Wang, Baole Ai, Bin Wen, Chaojie Mao, Chen-Wei Xie, Di Chen, Feiwu Yu, Haiming Zhao,
 552 Jianxiao Yang, Jianyuan Zeng, Jiayu Wang, Jingfeng Zhang, Jingren Zhou, Jinkai Wang, Jixuan
 553 Chen, Kai Zhu, Kang Zhao, Keyu Yan, Lianghua Huang, Xiaofeng Meng, Ningyi Zhang, Pandeng
 554 Li, Pingyu Wu, Ruihang Chu, Ruili Feng, Shiwei Zhang, Siyang Sun, Tao Fang, Tianxing Wang,
 555 Tianyi Gui, Tingyu Weng, Tong Shen, Wei Lin, Wei Wang, Wei Wang, Wenmeng Zhou, Wente
 556 Wang, Wenting Shen, Wenyuan Yu, Xianzhong Shi, Xiaoming Huang, Xin Xu, Yan Kou, Yangyu
 557 Lv, Yifei Li, Yijing Liu, Yiming Wang, Yingya Zhang, Yitong Huang, Yong Li, You Wu, Yu Liu,
 558 Yulin Pan, Yun Zheng, Yuntao Hong, Yupeng Shi, Yutong Feng, Zeyinzi Jiang, Zhen Han, Zhi-
 559 Fan Wu, and Ziyu Liu. Wan: Open and advanced large-scale video generative models. *CoRR*,
 560 abs/2503.20314, 2025. doi: 10.48550/ARXIV.2503.20314. URL <https://doi.org/10.48550/arXiv.2503.20314>.

561 Yi Wang, Yinan He, Yizhuo Li, Kunchang Li, Jiashuo Yu, Xin Ma, Xinyuan Chen, Yaohui Wang,
 562 Ping Luo, Ziwei Liu, Yali Wang, Limin Wang, and Yu Qiao. Internvid: A large-scale video-text
 563 dataset for multimodal understanding and generation. *arXiv preprint arXiv:2307.06942*, 2023.

564 Zhao Wang, Aoxue Li, Lingting Zhu, Yong Guo, Qi Dou, and Zhenguo Li. Customvideo: Customiz-
 565 ing text-to-video generation with multiple subjects. *arXiv preprint arXiv:2401.09962*, 2024.

566 Zhuoyi Yang, Jiayan Teng, Wendi Zheng, Ming Ding, Shiyu Huang, Jiazheng Xu, Yuanming
 567 Yang, Wenyi Hong, Xiaohan Zhang, Guanyu Feng, Da Yin, Yuxuan Zhang, Weihan Wang,
 568 Yean Cheng, Bin Xu, Xiaotao Gu, Yuxiao Dong, and Jie Tang. Cogvideox: Text-to-video diffu-
 569 sion models with an expert transformer. In *The Thirteenth International Conference on Learn-
 570 ing Representations, ICLR 2025, Singapore, April 24-28, 2025*. OpenReview.net, 2025. URL
 571 <https://openreview.net/forum?id=LQzN6TRFg9>.

572 Hu Ye, Jun Zhang, Sibo Liu, Xiao Han, and Wei Yang. Ip-adapter: Text compatible image prompt
 573 adapter for text-to-image diffusion models. *CoRR*, abs/2308.06721, 2023. doi: 10.48550/ARXIV.
 574 2308.06721. URL <https://doi.org/10.48550/arXiv.2308.06721>.

575 Yufan Zhou, Ruiyi Zhang, Jiuxiang Gu, Nanxuan Zhao, Jing Shi, and Tong Sun. SUGAR: subject-
 576 driven video customization in a zero-shot manner. *CoRR*, abs/2412.10533, 2024. doi: 10.48550/
 577 ARXIV.2412.10533. URL <https://doi.org/10.48550/arXiv.2412.10533>.

578
 579
 580
 581
 582
 583
 584
 585
 586
 587
 588
 589
 590
 591
 592
 593

A APPENDIX

A.1 DATA PIPELINE AND DATASET DETAILS

Our data pipeline comprises two essential stages:

(1) High-quality Subject Segmentation: We first perform robust subject segmentation to obtain precise masks of target subjects from raw video frames. Only those instances passing stringent quality criteria (size, clarity, semantic alignment) are retained for downstream processing.

(2) Cross-Paired Sample Construction: Rather than using segmented subjects with their original backgrounds, we construct **cross-paired** data samples. In this process, segmented subjects are composited with backgrounds or video clips from different, unrelated sources. This ensures that the model learns to disentangle subject identity from background and pose, thereby preventing it from overfitting to trivial copy-paste solutions or memorizing original contexts.

To further ensure dataset quality, we conducted a manual evaluation of the constructed dataset (segmentation subset). The results were favorable, owing to the use of high-confidence thresholds during the automated filtering stage — including strict localization thresholds in Grounding DINO, high CLIP similarity thresholds for category filtering, and high-confidence face detection for human subjects. The evaluation shows that the CLIP-based category filter achieves a success rate of over 92%, and face detection exceeds 95% accuracy, confirming the reliability of our pipeline.

For model robustness, we adopt a balanced training data ratio:

crop : segment : inpainting : redux = 1 : 5 : 3 : 1

where **crop** refers to cropped subjects, **segment** indicates high-quality segmentation, **inpainting** means removing backgrounds via generative inpainting, and **redux** refers to pose/motion augmentation. Importantly, we find that inpainting and redux samples serve primarily as guidance, so their proportions are kept moderate.

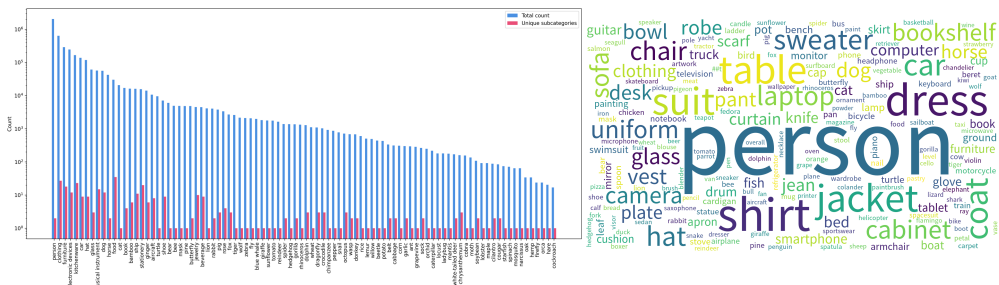


Figure 7: Statistics of our training dataset. .

Role of Cross-Pair Data. As illustrated in Fig. 6, training with only crop or segment inputs easily leads the model to memorize reference-image backgrounds and poses, resulting in copy-paste-like artifacts. Cross-paired samples mitigate this issue by explicitly breaking the correlation between subject identity and its original context, thereby enforcing stronger subject–background disentanglement and improving generalization.

To further quantify this effect, we conduct an ablation study on the proportion of cross-paired samples in training. As shown in Table A.1, introducing a moderate amount of cross-pairing (20–40%) significantly improves both *consistency* and *decoupling*. However, excessively large ratios (e.g., 80%) begin to degrade performance, suggesting that cross-pair data act as a regularizer: insufficient cross-pairing fails to eliminate context coupling, whereas overly aggressive cross-pairing suppresses high-fidelity subject signals required for S2V generation.

In addition, while **inpainting** and **redux** samples provide valuable supervisory signals—such as improving motion robustness and enhancing background flexibility—their contributions saturate when used excessively. Therefore, maintaining these samples at moderate proportions is crucial for preserving the balance between subject fidelity and generalization.

	Cross-Pair Ratio	Consistency	Decoupling
650	0%	0.670	0.297
651	20%	<u>0.692</u>	0.306
652	40%	0.708	<u>0.310</u>
653	60%	0.673	0.312
654	80%	0.664	0.307

Table 4: Impact of cross-pair ratios on subject consistency and subject–background decoupling.

A.2 DESIGN AND ANALYSIS OF R-ROPE

Motivation. Our goal is to investigate how a subject-to-video (S2V) model can more efficiently learn *extra visual conditions*—multiple reference images—during video generation. Existing approaches generally fall into two categories. (1) **Adapter-based methods** (e.g., VACE), which insert additional transformer layers for conditioning. Achieving competitive performance requires stacking many layers, introducing substantial increases in FLOPs and parameter count (e.g., adding $0.5 \times$ parameters to a 1.3B model). (2) **Sequence-concatenation methods** (e.g., Phantom), which keep base model parameters frozen and inject reference information by directly appending image tokens along the sequence dimension, thus retaining computational efficiency.

Motivated by these observations, we adopt *Sequence-Concatenation* for injecting subject conditions. We explored both *Channel-Concatenation* and *Sequence-Concatenation*. Although channel concatenation works well in I2V settings due to spatial alignment between image and video frames, it is less suitable for S2V, where alignment relies on semantic correspondence rather than spatial correspondence. Consistent with this hypothesis, our experiments (Table 6) show that channel concatenation and produces noticeably inferior S2V subject fidelity.

However, direct sequence concatenation introduces a clear issue: when reference images are appended as the last few frames, the model exhibits **subject overlap artifacts** (see Fig. 6), i.e.. This indicates that treating images as ordinary video frames disrupts the temporal generation prior. These observations motivate designing a positional encoding mechanism that explicitly distinguishes between *video tokens* and *reference-image tokens*. Rotary Position Embedding (RoPE) naturally provides the necessary degrees of freedom.

Design of R-RoPE. We extend RoPE by applying deterministic shifts along the spatial (H/W) and temporal (T) index only to reference-image tokens, while keeping video tokens untouched. The design follows three principles: (1) video and image tokens must be easily distinguishable; (2) different reference images should be separable; (3) no artificial temporal continuity should be implied among images.

Evaluated Variants. To systematically examine which indices carries meaningful conditioning signals, we evaluate the following R-RoPE variants:

Method	Subject	Background
ShiftW&H	0.708	0.310
ShiftW&H w/o overlap	0.690	0.296
Staggered Negative Time Shift (T = -3, -2, -1)	0.683	0.276
Fixed-Time Encoding (T = -1)	0.644	0.298
Future-Shifted Time Encoding (T = +1, +2, +3)	0.667	0.300
Channel-Concat	0.632	0.285

Table 5: Extended evaluation of R-RoPE variants for S2V conditioning. Metrics correspond to subject consistency (left) and background consistency (right).

- **Spatial-only variants:** **ShiftW&H**: all reference images share identical spatial shifts. **ShiftW&H w/o overlap**: each reference image receives an independent spatial shift, removing overlap in the (H,W) RoPE indices.

702
 703
 704
 705
 706
 707
 708
 709
 710
 711
 712
 713

- **Temporal-shift variants:** We define three families of temporal manipulations, each corresponding to how the t -indices of reference images are assigned: Here, T denotes the pseudo-time index along the temporal dimension, with negative values representing positions before the video sequence, and positive values after it.
 - **Fixed-Time Encoding ($T = -1$):** for each reference subject, all associated images are assigned a fixed negative time index $T = -1$.
 - **Staggered Negative Time Encoding ($T = -3, -2, -1$):** for each reference subject, the images are assigned progressively earlier negative time indices, e.g., $T = -3, -2, -1$.
 - **Future-Shifted Time Encoding ($T = +1, +2, +3$):** for each reference subject, the images are assigned time indices following the final frame of the video sequence, e.g., $T = N + 1, N + 2$, where N is the number of video frames.

714
 715
 716
 717
 718
 719
 720
 721
 722
 723
 724

Results. Table A.2 summarizes the quantitative performance for all newly evaluated variants. The **spatial-only R-RoPE with shared H/W shifts** yields the best subject fidelity and background consistency. In contrast, **temporal shifts consistently underperform**: either fixing the time index, assigning staggered negative indices, or shifting references into future frames all introduce modality bias that degrades the model’s ability to learn subject semantics.

725
 726
 727
 728
 729
 730
 731
 732
 733
 734
 735
 736
 737
 738
 739
 740
 741
 742
 743
 744
 745
 746
 747
 748
 749
 750
 751
 752
 753
 754
 755

Summary. Overall, the extended analysis reveals: (1) S2V requires semantic-level conditioning, making sequence concatenation more suitable than channel concatenation; (2) positional embeddings are critical to prevent reference-image duplication artifacts; (3) **spatial-only R-RoPE with shared H/W shifts is the most stable and effective design**, while temporal shifts introduce modality inconsistency and consistently degrade performance.